Available online at www.sciencedirect.com
SCIENCE DIRECT
Virology 350 (2006) 171–183
VIROLOGY
www.elsevier.com/locate/yviro

Infectious cDNA transcripts of *Maize necrotic streak virus*: Infectivity and translational characteristics

Kay Scheets [a,*], Margaret G. Redinbaugh [b]

[a] *Department of Botany, 104 Life Sciences East, Oklahoma State University, Stillwater, OK 74078, USA*
[b] *USDA-ARS, Corn and Soybean Research and Department of Plant Pathology, The Ohio State University, OARDC, 1680 Madison Avenue, Wooster, OH 44691, USA*

Received 5 December 2005; returned to author for revision 11 January 2006; accepted 6 February 2006
Available online 20 March 2006

Abstract

Maize necrotic streak virus (MNeSV) is a unique member of the family Tombusviridae that is not infectious by leaf rub inoculation and has a coat protein lacking the protruding domain of aureusviruses, carmoviruses, and tombusviruses (Louie et al., Plant Dis. 84, 1133–1139, 2000). Completion of the MNeSV sequence indicated a genome of 4094 nt. RNA blot and primer extension analysis identified subgenomic RNAs of 1607 and 781 nt. RNA and protein sequence comparisons and RNA secondary structure predictions support the classification of MNeSV as the first monocot-infecting tombusvirus, the smallest tombusvirus yet reported. Uncapped transcripts from cDNAs were infectious in maize (*Zea mays* L.) protoplasts and plants. Translation of genomic and subgenomic RNA transcripts in wheat germ extracts indicated that MNeSV has a 3′ cap-independent translational enhancer (3′CITE) located within the 3′ 156 nt. The sequence, predicted structure, and the ability to function in vitro differentiate the MNeSV 3′CITE from that of *Tomato bushy stunt virus*.

Keywords: Tombusvirus; Infectious transcripts; *Maize necrotic streak virus*; MNeSV; Cap-independent translation; Translational enhancer

Introduction

Maize necrotic streak virus (MNeSV) is a monopartite single-stranded positive sense RNA virus, and partial genome sequence analysis showed it to be related to members of the family Tombusviridae (Louie et al., 2000). The genome organization of MNeSV was found to be similar to that of tombusviruses and aureusviruses with five open reading frames (ORFs). Nonstructural proteins encoded by MNeSV were most similar to tombusviruses, even though the estimated size (~4.3 kb) of virion RNA (vRNA) was closer to that of aureusviruses. Analysis of the predicted 27.4 kDa coat protein (CP) of MNeSV indicated that it did not contain the protruding domain found on tombusvirus and aureusvirus CPs and was most closely related to CPs of necroviruses. The virion size of 32 nm was closer to that of tombusviruses (32–35 nm) (Lommel et al., 2005b) than necroviruses (28 nm) (Lommel et al., 2005a). Similarly to tombusviruses, no insect vector of MNeSV was identified among eight insect species tested (Louie et al., 2000). A characteristic of MNeSV that differentiated it from previously identified tombusviruses was that the virus could not be transmitted by leaf rub inoculation (Louie et al., 2000). However, MNeSV readily infected maize (*Zea mays* L.) via vascular puncture inoculation (VPI) of seeds.

Several species of dicot-infecting tombusviruses have been used to study various aspects of the virus life cycle: replication in vivo (Fabian et al., 2003; Ray et al., 2003; Wu et al., 2001), in vitro (Nagy and Pogany, 2000; Panavas et al., 2002), and in yeast (Panavas and Nagy, 2003; Pantaleo et al., 2003); recombination and production of defective interfering-RNAs (DI-RNAs) (Burgyan et al., 1991; Reade et al., 1999; Scholthof, K. et al., 1995); transcription (Choi and White, 2002; Choi et al., 2001; Lin and White, 2004); in vivo translation (Fabian and White, 2004; Wu and White, 1999); cell-to-cell and long-distance movement (Chu et al., 2000; Scholthof, H. et al., 1995); initiation and suppression of gene silencing (Havelda et al.,

* Corresponding author. Fax: +1 405 744 7074.
E-mail addresses: kay.scheets@okstate.edu (K. Scheets), redinbaugh.2@osu.edu (M.G. Redinbaugh).

0042-6822/$ - see front matter © 2006 Elsevier Inc. All rights reserved.
doi:10.1016/j.virol.2006.02.004

2003; Qiu et al., 2002); and fungal transmission (McLean et al., 1994). The similarity of MNeSV to tombusviruses suggested that it might be the first monocot-infecting tombusvirus and could thus provide a very useful tool to compare aspects of the tombusviral life cycle in a monocot system.

The genomes of viruses in the family Tombusviridae are uncapped and do not contain poly(A) tails, two structures required for efficient translation of most eukaryotic mRNAs. For plant mRNAs, the ^{m}7GpppN cap is bound by initiation factor eIF4F or eIFiso4F, the poly(A) tail is coated by poly(A) binding protein, and both proteins bind to additional initiation factors to form a circular structure which efficiently recruits the 40S ribosome subunit (Kawaguchi and Bailey-Serres, 2002). Many viruses use alternative 5′ and/or 3′ structures to efficiently translate their mRNAs. In the family Tombusviridae, 3′ translational enhancers (3′TEs) have been previously identified in *Tomato bushy stunt virus-C* (TBSV-C) (Wu and White, 1999), the necroviruses *Tobacco necrosis virus-A* (TNV-A) and TNV-D (Meulewaeter et al., 2004; Shen and Miller, 2004) and their satellite virus STNV (Danthinne et al., 1993; Timmer et al., 1993), the dianthovirus *Red clover necrotic mosaic virus* (Mizumoto et al., 2003), and the carmoviruses *Turnip crinkle virus* (Qu and Morris, 2000) and *Hibiscus chlorotic ringspot virus* (Koh et al., 2002). TBSV does not naturally infect cereals, and its 3′ cap-independent translational enhancer (3′CITE) is active in cucumber protoplasts but not in wheat germ extract (WGE) (Wu and White, 1999). As a monocot-infecting tombusvirus, we hypothesized that MNeSV might provide a tool for analyzing cap-independent translation of a tombusvirus in WGE, a system used for the well-studied 3′TE of *Barley yellow dwarf virus*-PAV (BYDV-PAV) (Allen et al., 1999) and other viruses.

In this paper, we report the completed sequence of MNeSV and the construction of infectious transcript cDNAs. We also mapped the two subgenomic RNAs (sgRNAs) and identified predicted secondary structures in MNeSV genomic RNA (gRNA) similar to those found for dicot tombusviruses. Lastly, we have identified a cap-independent translational enhancer in the 3′ untranslated region (UTR) of MNeSV that functions on gRNA and sgRNAs in WGE. These results indicate that MNeSV should be classified as a tombusvirus.

Results

MNeSV genome sequence and secondary structure

Analysis of the initial sequence data for MNeSV suggested that about 10% of the viral sequence was missing based on the vRNA size estimate. Two approaches were used to complete the sequence of the 5′ end of the MNeSV genome. First, cDNAs synthesized with RNA ligase-mediated rapid amplification of cDNA ends (RLM-RACE) of vRNA that was not pretreated with calf intestinal phosphatase (CIP) or tobacco acid pyrophosphatase (TAP) were cloned into a plasmid vector and sequenced (Table 1). No cDNA could be amplified from vRNA that was pretreated with CIP followed by TAP before the RNA ligation reaction (data not shown), indicating that the vRNA was uncapped. Four cDNAs with the same sequence and one with a deletion of at least two A's corresponding to the 3′ end of the RNA oligomer, which terminated with GAAA, were identified (Table 1). These data suggested the RNA oligomer was partially deteriorated. Using an alternative strategy for RACE, cDNA synthesized from vRNA was C-tailed then used for PCR. The sequence of these cloned PCR products indicated the 5′ viral sequence was AGAUAU (Table 1). This sequence was consistent with results of primer extension analysis which produced cDNAs one base longer than the GATAT found in RLM-RACE-derived clones (Fig. 1). Thus, it is likely that the RNA primer or the vRNA was degraded prior to ligation in the clones derived from RLM-RACE and that the 5′ sequence of the MNeSV RNA is AGAUAU. This sequence is consistent with that of many tombusviruses (White and Nagy, 2004). The sequences of the 5′ RACE products indicated that there were 28 additional nt at the 5′ end of the viral genome relative to the previously published sequence (Louie et al., 2000). In addition, sequences of the RACE products indicated that the residue at nt 88 of the full-length sequence was a C rather than the U reported earlier.

Table 1
Sequences of the 5′ end of the MNeSV vRNA determined using RACE

Method [a]	# clones [b]	Sequence [c]
RLM-RACE	4	atgaaaGATAT
RLM-RACE	1	atga GATAT
5′ RACE	2	gggggAGATAT
Tombusvirus consensus [d]		AGAAAU

[a] The sequences of cDNAs were obtained using the RLM-RACE kit (Ambion) with untreated vRNA or a 5′ RACE kit (Invitrogen) using total RNA.
[b] The number of cDNAs showing the indicated sequence.
[c] Sequences corresponding to viral RNA are indicated in uppercase letters, and those corresponding to the RNA oligomer or complement of the C-tail are indicated in lower case letters.
[d] The dicot tombusvirus consensus vRNA 5′ terminal sequence (White and Nagy, 2004).

The initial MNeSV sequence data terminated within ORF5, indicating that some of the coding region and the 3′UTR were missing. The 3′ end of the MNeSV genome was obtained using anchored cDNA cloning (Weng and Xiong, 1995) with an upstream primer corresponding to nt 3623–3647 of the previously published MNeSV sequence (nt 3651–3675 of the complete sequence, GenBank accession number AF266518). Three cDNAs were sequenced, and two positions showed transitions at nt 3909 (A/G) or 3988 (C/T). Analysis of the resulting data indicated that the previously published partial sequence contained a duplicated fragment (nt 2188–2290 of the viral genome) inserted after nt 3832. After accounting for the duplication, 258 nt of additional sequence was identified in the anchored cDNA clones. Thus, the complete sequence of MNeSV is 4094 nt which is about 660 nt smaller than most dicot tombusviruses and is 482 nt smaller than *Cucumber Bulgarian latent virus* (CBLV GenBank accession number AY163842).

With the sequence completed, we reevaluated the positions and sizes of the ORFs, the similarity of encoded proteins and RNA, and predicted RNA secondary structures for comparison

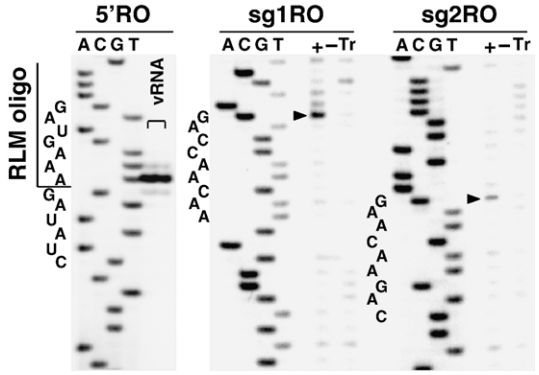

Fig. 1. Primer extension mapping of the 5′ termini of the MNeSV vRNA and sgRNAs. Primers (see Materials and methods for sequences) used for each reaction are listed at the top of the lanes. RNA from two different virion preparations was used for extension with the 5′RO primer. The products were run next to a sequencing ladder for a 5′ RLM-RACE cDNA using the same primer. To identify the 5′ ends of the viral sgRNAs, total RNA from infected (+) or healthy (−) plants and t8-6 RNA (Tr) were used as templates, and the sequencing ladder was generated using p8-6. Arrowheads mark the sgRNA 5′ ends, and all sequences represent (+) RNAs.

to other tombusviruses (Figs. 2 and 3A). The 122 nt MNeSV 5′ UTR was similar in size to the 134 nt 5′UTR of CBLV and was 44 nt shorter than that of TBSV-C (GenBank accession number M21958). ClustalW alignment of ten tombusviruses showed that MNeSV's 5′UTR had 73% identity with CBLV and lower similarity (45–57%) to other tombusviruses. The sequence similarity was greatest near the p30 start codon where identical stretches of 10 and 13 nt were found in MNeSV and all dicot tombusviruses (Fig. 2A and data not shown). RNA folding analysis was performed to determine whether MNeSV's 5′UTR contained structural features characteristic of a tombusvirus despite the low sequence similarity. RNA folding analysis using STAR (Gultyaev et al., 1995) and mfold (Zuker, 2003) predicted that the MNeSV 5′UTR contains secondary structures similar to those shown to be important for TBSV replication and predicted to be found in other tombusviruses (Ray et al., 2003; Wu et al., 2001) (Figs. 2 and 3A). The predicted structures include a 5′ T-shaped domain (TSD), a simple stem loop (SL), a downstream domain (DSD), and a potential pseudoknot between the TSD loop and bases immediately preceding the p30 start codon (Fig. 2A). Although Fig. 2A represents the fourth lowest energy mfold structure (0.37 kcal/mol higher than lowest energy structure), it most closely resembles the TBSV structure, including identical single-stranded sequences in the DSD that correspond to intervening sequence 5/6 (is5/6), bulge 1 (B1), and bulge 2 (B2) of TBSV (Ray et al., 2003). STAR predicted a similar structure (data not shown).

The RNA sequence of MNeSV ORF1 had low identity (43–59%) with ORF1 from dicot tombusviruses largely due to deletion(s) in MNeSV that occur about one third of the way (nt 407 to 434) from the 5′ end of the ORF (data not shown). ORFs 2, 4, and 5 of MNeSV showed 72–77% identity with their dicot tombusviral counterparts, bracketing the dissimilar necrovirus-like CP gene (ORF3). The sizes of proteins expected from the first ORF and its readthrough product (ORF2) indicated that the 5′ portion of MNeSV encodes proteins of 30 and 88.6 kDa (Fig. 3A) instead of 33.3 and 92.1 kDa as originally reported (Louie et al., 2000). Additionally, the readthrough portion of p89 had 80–82% identity with the homologous protein regions encoded by dicot tombusviruses, giving an overall identity of 64–74%

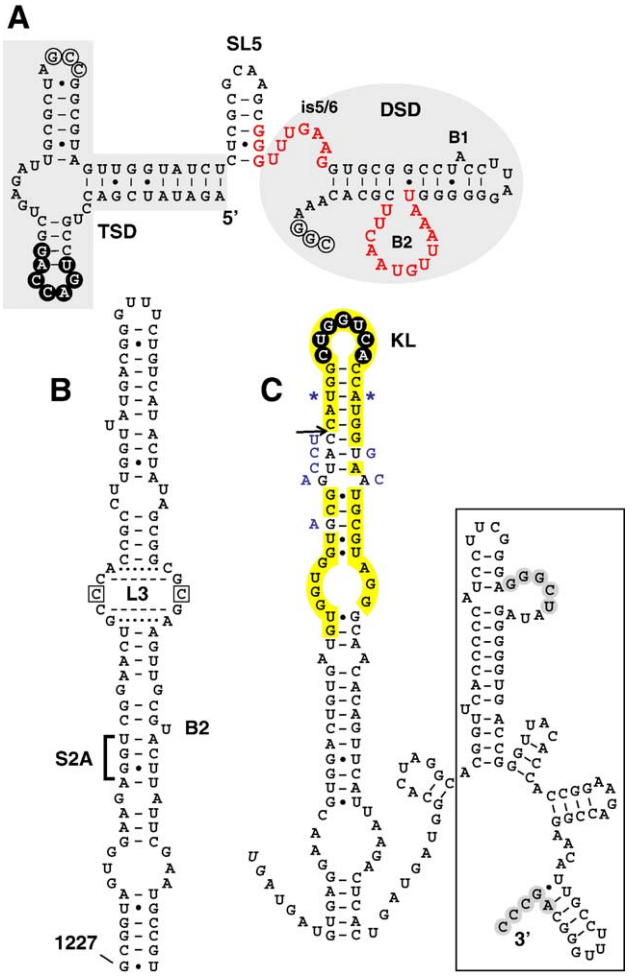

Fig. 2. Predicted RNA folding structures for the 5′ UTR, 3′UTR, and putative internal replication element of MNeSV. (A) 5′UTR structure that most closely resembles the regions identified in TBSV (Ray et al., 2003), predicted as fourth lowest energy folding by mfold version 3.1 (Zuker, 2003). Sequences that are identical in all tombusviruses are red letters. The T-shaped domain (TSD) and downstream domain (DSD) are highlighted in gray. The central stem loop (SL5) corresponds to the fifth stem loop in TBSV. The intervening sequence (is5/6), bulge 1 (B1), and bulge 2 (B2) regions of the DSD are marked. Bases in open circles may base pair like the pseudoknot in TBSV, and bases complementary to the loop in the MNeSV 3′UTR are white letters in black circles. (B) The single structure predicted by mfold version 3.1 for nt 1227–1324, the putative internal replication enhancer. The large loop (L3) with a CC mismatch (boxed Cs) has potential Watson/Crick (dashed) or non-Watson/Crick (dotted) base pairs marked, and the bulge (B2) and stem (S2A) correspond to regions in the alternative structure of the region II hairpin of TBSV DI-RNA (Monkewich et al., 2005). (C) The lowest energy 3′UTR structure predicted by mfold version 2.3 at 37 °C and 28 °C. The p21 stop codon is italicized. An arrow marks the 3′ end of *Asp718*I-truncated transcripts. Yellow-highlighted sequences are identical to sequences in CBLV, and blue letters show differences for the CBLV sequence. The blue asterisks represent one nt deletions in CBLV. Bases complementary to the first TSD loop in the MNeSV 5′UTR are white letters in black circles, while gray circles mark bases in the putative replication silencer element (RSE) and its complement at the 3′ end (Fabian et al., 2003). A rectangle encloses the region with high sequence identity to other tombusviruses.

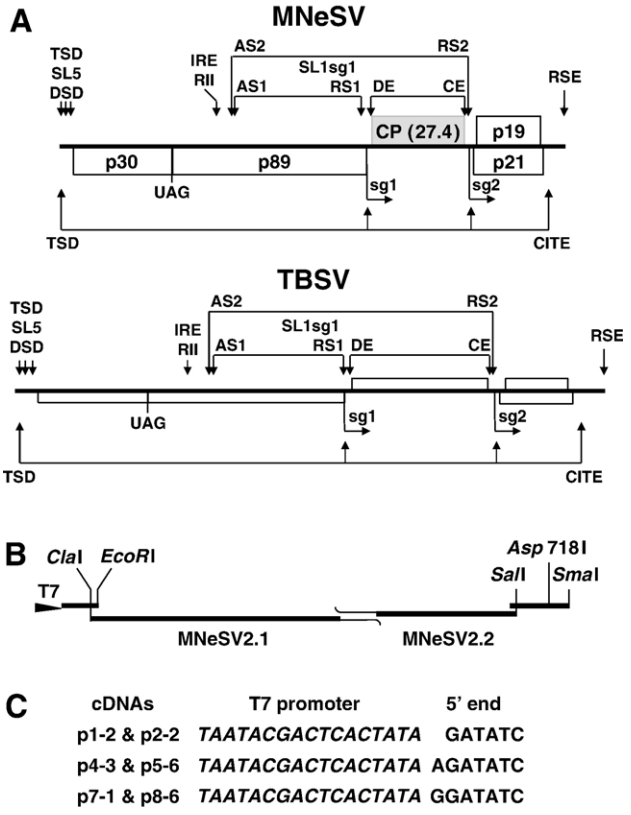

Fig. 3. Comparison of genome maps of MNeSV and TBSV and construction of full-length MNeSV cDNAs. (A) Open boxes represent major ORFs, and the leaky stop codons (UGA) found in the RdRp ORFs are indicated. sgRNA start sites (sg1 and sg2) are marked by bent arrows below the genomes. The MNeSV nonhomologous CP ORF is represented as a gray box. The locations of regulatory elements are marked by arrows. Long distance base-pairing motifs affecting transcription have connected arrows above the genomes, while long distance base-pairing motifs affecting translation have connected arrows below the genomes. Replication regulators include the T-shaped domain, stem loop 5, downstream domain (TSD, SL5, DSD) (Ray et al., 2003; Wu et al., 2001), internal replication element RII (IRE RII) (Monkewich et al., 2005), and replication silencing element (RSE) (Fabian et al., 2003; Pogany et al., 2003). sgRNA regulatory elements include activator sequence-1, stem loop 1sg1, receptor sequence-1 (AS1, SL1sg1, RS1) (Choi and White, 2002), AS2, RS2 (Lin and White, 2004), distal element, core element (DE, CE) (Zhang et al., 1999), and cap-independent translational enhancer (CITE) (Fabian and White, 2004; Wu and White, 1999). The TBSV figure is modified from Lin and White (2004). (B) The four cDNA fragments used to construct full-length MNeSV cDNAs are indicated with heavy lines. The ssDNA overlap regions of MNeSV2.1 and MNeSV2.2 are shown with thin lines. The locations of restriction sites used for cDNA construction and transcription template linearizations are marked. (C) The sequences at the 5′ ends of the transcription template cDNAs are shown next to the T7 RNA promoter sequence which is italicized.

for p89 compared to other tombusviruses instead of the 40–42% originally reported. Within ORF2, the sequence (nt 1227–1324) corresponding to the internal replication element (IRE RII) of TBSV was predicted to fold into a long hairpin with loops and bulges (Fig. 2B). The structure included a CC mismatch which was critical for in vitro binding of TBSV p33 (Pogany et al., 2005) and replication of DI-RNAs in cucumber protoplasts (Monkewich et al., 2005) and yeast (Pogany et al., 2005). The MNeSV structure is more similar to the alternative structure predicted for TBSV since it included a bulge (B2) instead of a loop and the alternative base-pairing partners that form a four base pair stem section (S2A) instead of a three base pair section (Monkewich et al., 2005). The completed sequence of the 3′ end showed that the two nested ORFs encode proteins of 21.4 kDa and 19 kDa (Fig. 3A) with different carboxy-terminal sequences than originally reported. p21 had 68–73% sequence identity to the p22 proteins of tombusviruses, while MNeSV's p19 had 54–59% identity with other tombusvirus p19 proteins as determined from ClustalW analysis (data not shown).

The 3′UTR was found to be 197 nt long, about 55% of the length of those found in most other tombusviruses. No ORF longer than 23 amino acids (nt 3891 to 3959) was found in this region. Compared to the 5′UTR, the 3′UTR of MNeSV showed less overall similarity to 3′UTRs of other tombusviruses largely due to the size differences, with the most similarity (51% identity) to CBLV using ClustalW analysis (data not shown). The 5′ half of the MNeSV 3′UTR was least similar to the same region in other tombusviral 3′UTRs, and there was no overall conservation of secondary structure as this portion of the MNeSV 3′ UTR was predicted to fold into a long stem loop with four bulges (Fig. 2C). This differs from the Y-shaped structure predicted for most dicot tombusviruses and identified as the location of the 3′ CITE of TBSV (Fabian and White, 2004). Using default program settings in mfold and STAR, none of the predicted structures for MNeSV contained a Y-shaped stem loop (data not shown). A 44 nt sequence on the outer half of the MNeSV long SL showed 79% identity (Fig. 2C) to CBLV and 47–54% identity with the upstream arm region (SL-B) of the Y-shaped domain of the other dicot tombusviruses (data not shown). The seven nt of the terminal "kissing loop" (KL), which are complementary to nt in the first loop in the 5′UTR TSD (Figs. 2A and C), are identical to CBLV and one nt different from the six nt loop of the other tombusviruses. The last 90 nt of MNeSV showed 65–77% sequence identity (ClustalW) to the terminal sequences of dicot tombusviruses making this the largest conserved region in either UTR. Both the STAR and mfold programs predicted stem loop structures at the 3′ terminus similar to those mapped for TBSV or predicted for other tombusviruses (Fig. 2C). Furthermore, sequences and structures associated with the tombusvirus replication silencer element (RSE) are conserved (Fabian et al., 2003; Pogany et al., 2003). Thus, there was a remarkable conservation of motif order (Fig. 3A) and sequence between the MNeSV genome and those of other tombusviruses.

Identification of sgRNA transcription initiation sites and putative regulatory sequences

During tombusvirus replication, the CP is expressed from a large sgRNA, and the two overlapping 3′ ORFs are expressed from a smaller sgRNA. Primer extension analysis of total RNA from MNeSV-infected and healthy maize plants indicated the presence of sgRNAs of 1607 and 781 nt initiating at nt 2488 and 3314, respectively (Fig. 1). Northern blot analysis of RNA from infected maize Black Mexican Sweet (BMS) suspension culture protoplasts confirmed the presence of two sgRNAs (Fig. 4). Complementary seven nt sequences that differ by one nt from activator sequence-1 (AS-1) and receptor sequence-1 (RS-1),

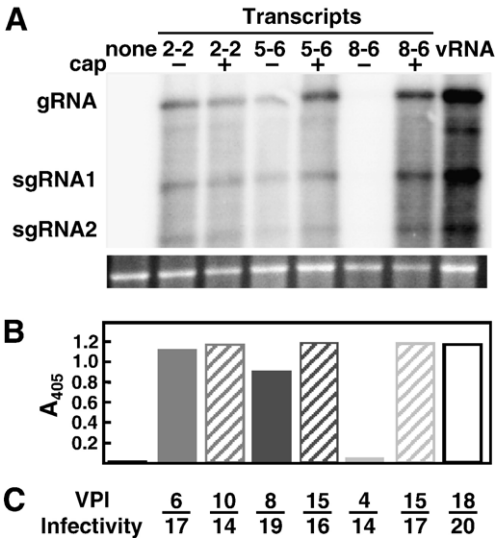

Fig. 4. Infectivity of in vitro synthesized MNeSV transcripts and vRNA in protoplasts and plants. BMS protoplasts were inoculated with vRNA, uncapped (−), or capped (+) transcripts from three cDNA clones or mock-inoculated (none), and samples for total RNA and CP were collected at 48 h post-inoculation for analysis. (A) Phosphorimage of a Northern blot to detect (+) RNA with a 3′ end probe. Locations of genomic RNA (gRNA) and sgRNAs are marked. The ethidium-bromide-stained 18S rRNA below the phosphorimage shows loading levels. (B) CP accumulation in protoplasts assayed by PAS-ELISA. (C) Maize seeds were inoculated by VPI with uncapped or capped transcripts or infected plant extract (far right), and seedlings were monitored for infection. Not all seeds germinated after VPI, so the fraction represents number infected/number germinated and is the sum of two independent experiments.

two widely separated components that base pair as part of the sgRNA1 promoter for TBSV (Choi and White, 2002), were identified in MNeSV at nt 1476–1782 and nt 2478–2484 (Fig. 3A). Sequence comparisons indicated that the 11 nt immediately upstream of the sgRNA2 start site is identical to the TBSV sequences for RS-2 (nt 3303–3308) and core element-C (CE-C) (nt 3309–3313), which are essential for sgRNA2 accumulation in TBSV (Choi et al., 2001; Lin and White, 2004; Zhang et al., 1999). In addition, a sequence complementary to RS-2 and identical to the AS-2 of TBSV was found at nt 1436–1442. In TBSV, these sequences comprise part of the sgRNA2 promoter (Lin and White, 2004). Complementary sequences in positions analogous to the TBSV sgRNA2 regulatory sequences distal element-A (DE-A) and CE-A (Choi et al., 2001; Zhang et al., 1999) were identified at nt 2510–2516 and 3293–3299, flanking the CP start and stop codons, respectively. Examination of the sgRNA 5′UTRs indicated that they contain sequences complementary to the KL region in the 3′UTR (Fig. 5). For sgRNA1, two complementary sequences were found, and, in sgRNA2, complementary sequences were identified just upstream of both the p21 and p19 start codons (Fig. 5). These results suggest that genomic elements required for transcription of MNeSV sgRNAs are similar to those of other tombusviruses.

Construction and infectivity of MNeSV transcription clones

Because of initial ambiguities regarding the 5′ nucleotide of MNeSV (Table 1) and sequence differences in the 3′UTR, plasmids representing six possible sequence variants were constructed such that each 5′ end was immediately downstream of a T7 RNA polymerase promoter and the 3′ end was upstream of a unique *Sma*I site (Figs. 3B and C). Three different 5′ end sequences were made based on the results of RACE experiments (Fig. 3C). The 3′ ends contained either a G and a C (p1-2, p4-3, p7-1) or an A and a T (p2-2, p5-6, p8-6) at nt 3909 and 3988, respectively, representing the variable bases found in the 3′ cDNAs. Transcripts synthesized in vitro from these cDNAs are identified throughout the text by replacing the "p" in the plasmid name with a "t".

To determine the infectivity of the cDNAs, uncapped transcripts were synthesized and used to inoculate BMS protoplasts. The protoplasts were analyzed for accumulation of viral RNAs and CP 48 h post-inoculation (hpi). Transcripts initiating with GAUAU and AGAUAU (t1-2, t2-2, t4-3, and t5-6) were readily infectious in protoplasts as shown by the accumulation of gRNA, sgRNAs, and CP, and there was no apparent effect of the base changes in the 3′UTRs on the accumulation of MNeSV RNAs in protoplasts (Fig. 4 and data not shown). Inoculation of protoplasts with transcripts initiating with GGAUAU (t7-1 and t8-6) produced extremely low but detectable CP accumulation (Fig. 4 and data not shown). Additionally, sgRNAs as well as gRNA were visible for t7-1 and t8-6 inoculations when the phosphorimage data were compressed to levels that "overexpose" the images for all other positive RNA signals (data not shown), indicating that very low levels of replication occurred.

Initial VPI inoculations of maize seeds were performed with RNAs generated from transcription reactions containing ^{m}7GpppGTP, and all six transcripts produced similar numbers of infected plants (Fig. 4 and data not shown). Our results with RLM-RACE showed that the MNeSV vRNA, like dicot tombusviruses, is not capped. To further examine the effect of capping on the infectivity of MNeSV, capped and uncapped transcripts were used to inoculate both protoplasts and seeds. Inoculation of protoplasts with capped and uncapped t2-2, t5-6, and t8-6 showed that, although uncapped t8-6 was infectious at very low levels, inoculation with capped t8-6 increased the infectivity to levels seen with capped t2-2 and t5-6 (Fig. 4).

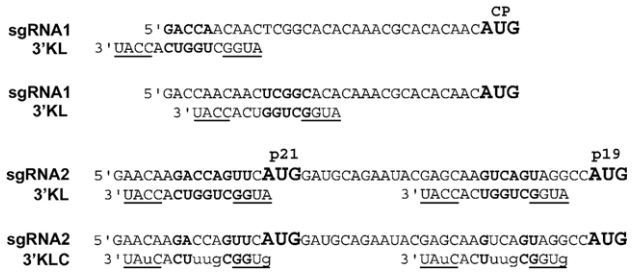

Fig. 5. Complementarity of sequences in the MNeSV sgRNA 5′ ends and the 3′ UTR kissing loop. The 5′ ends of sgRNA1 and sgRNA2 including the UTRs and start codons for CP, p21, and p19 are aligned with the 15 nt sequence containing the kissing loop (3′KL). The start codons are indicated in larger bold font. Complementary sequences are bold, and bases that are paired in the stem in Fig. 2C are underlined. The same alignment is shown for the transcript from pNsg2-KLC (3′KLC), and mutated bases are shown in lower case. The underlined regions containing mutations in pNsg2-KLC are predicted to base pair in the stem the same as wild type.

Capped t2-2 and t5-6 were only moderately more infectious than their uncapped transcripts (Fig. 4 and data not shown). Note that t5-6 capped transcription reactions produced a mixture of uncapped t5-6 and capped t2-2 RNAs.

To determine whether capped and uncapped versions of t2-2, t5-6, and t8-6 showed differential infectivity in plants as well as protoplasts, capped and uncapped transcripts were inoculated to maize seeds via VPI. All plants that became infected showed the same rate of symptom appearance and symptom severity, regardless of whether they were inoculated with transcripts or MNeSV-infected plant extract. Both uncapped and capped transcripts of all three cDNAs infected plants, but capped transcripts infected a larger fraction (Fig. 4). While differences in the infectivity in capped vs. uncapped transcripts were apparent after protoplast inoculation and VPI, the difference in infectivity of capped vs. uncapped t8-6 was less after VPI. This may reflect the effect of the time of analysis or the relatively small numbers of samples analyzed.

To ensure that the observed differences in infectivity of p8-6 were not due to unexpected mutations, inserts of both p2-2 and p8-6 were completely sequenced to confirm that the only difference between them was the extra G at the 5′ end of the p8-6 insert. Furthermore, the differential replication of the capped and uncapped forms of t8-6 in protoplasts was confirmed using inocula derived from different plasmid and transcript preparations (data not shown). These data indicated that, in protoplasts, uncapped transcripts initiating with GGAUAU were much less infectious than transcripts initiating with GAUAU and AGAUAU, and all capped transcripts had similar infectivity which was slightly better than uncapped t2-2 and t5-6 infectivity. p2-2 was selected as the "wild type" transcription cDNA for MNeSV since uncapped t2-2 was highly infectious in protoplasts and plants, and its 5′G allowed for more efficient in vitro synthesis compared to the equally infectious p5-6. Thus, uncapped transcripts from p2-2 contain nt 2-4094 of the GenBank (AF266518) sequence. These data indicate that, like tombusvirus transcripts, uncapped MNeSV transcripts are infectious in plants. Furthermore, there is some lack of discrimination for the 5′ nucleotide of the infectious transcripts in plants, but in protoplasts, the infectivity of uncapped transcripts initiating with GG is greatly reduced.

In vitro synthesis of viral proteins from MNeSV transcripts

To confirm the translation strategy and determine the relative mobility of the proteins encoded in MNeSV, transcripts for gRNA and sgRNAs were synthesized and translated in vitro. Plasmids pNsg1 and pNsg2 encoding sgRNA1 or sgRNA2, respectively, downstream of a T7 RNA polymerase promoter were constructed and used to synthesize sgRNA transcripts with the subgenomic 5′ and 3′ ends determined in earlier experiments. Equimolar amounts of vRNA, uncapped t2-2, and uncapped sgRNA transcripts were used for in vitro translations in WGE in the presence of ^{35}S-methionine, and equal volumes of the reactions were analyzed by SDS-PAGE (Figs. 6 and 7). The five MNeSV-encoded proteins migrated with apparent molecular weights within 5–10% of the molecular weights calculated from

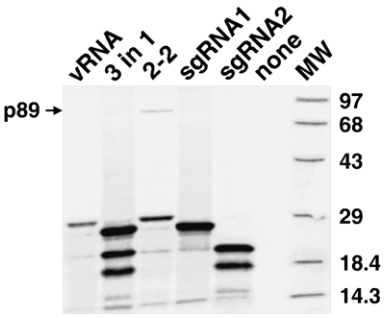

Fig. 6. In vitro translation products of MNeSV vRNA and uncapped gRNA or sgRNA transcripts from wheat germ extracts. Water (none) or 0.5 pmol of vRNA (vRNA), full-length transcripts of gRNA (2-2), or sgRNAs (sgRNA1 and sgRNA2) were used. For one translation, t2-2 and the two sgRNA transcripts (3 in 1) were mixed before adding the RNAs to the WGE. Equal volumes of translation reactions were separated by SDS-PAGE, electroblotted to nitrocellulose, and exposed to a phosphorimager. Sizes of molecular weight markers (MW) are on the right, and the location of p89 is marked with an arrow.

the amino acid composition. The major product of vRNA and t2-2 was the 30 kDa protein, and in vitro translation of t2-2 also produced p89 at about 2% of the level of p30. p89 was not detected in any in vitro translation using vRNA (Fig. 7 and data not shown). Lack of p89 synthesis from vRNA may have been due to the presence of an inhibitor that copurified with vRNA or a smaller fraction of full-length RNA in vRNA preparations compared to transcripts. CP and p21 were minor products in translation reactions programmed with vRNA and t2-2, as were proteins corresponding in size to those expected from initiation at some internal methionines in ORFs 1 and 2 (Figs. 6 and 7 and data not shown). The primary translation product from tNsg1 was the 27 kDa CP, while tNsg2 produced 21 kDa and 19 kDa proteins as expected (Fig. 6). These data are consistent with MNeSV encoding five proteins of the sizes predicted from the ORFs.

Cap-independent in vitro translation of MNeSV transcripts in wheat germ extracts

WGE shows a marked discrimination for translation of most capped RNAs compared to their uncapped counterparts, but some CITEs functionally replace the ^{m}7GpppN cap. To determine whether MNeSV encodes a 3′CITE that is active in WGE, in vitro translations of the capped and uncapped t2-2 RNAs were compared with translations of transcripts truncated to remove the KL by digestion of p2-2 with *Asp718*I prior to transcription (t2-2Δ3′) (Figs. 2C and 3B). More than twice as much p30 was synthesized when capped t2-2 was translated compared to translation of uncapped t2-2 (Fig. 7). Truncated uncapped transcripts produced 8- to 50-fold less p30 than uncapped t2-2 (Fig. 7). In contrast, translation of capped t2-2Δ3′ produced about 50% as much p30 as capped t2-2. These data showed that the 3′ 156 nt contains a CITE that functionally replaces a 5′ cap and suggested that it may also provide an additional function, possibly as a poly(A) replacement (Guo et al., 2000). The activity of the 3′CITE was also tested for sgRNA translations. Similarly to the full-length transcripts, translation rates of capped sgRNA transcripts were higher than translation of

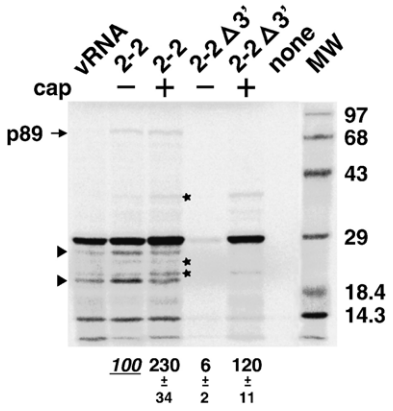

Fig. 7. Effects of ^{m}7GpppG caps and 3′ truncations on translation of MNeSV gRNA transcripts in wheat germ extracts. Water (none) or 0.5 pmol of vRNA, uncapped (−), or capped (+) full-length transcripts (2-2) or transcripts missing the 3′ 156 nt (2-2Δ3′) were used. Sizes of molecular weight markers (MW) are on the right, and the proteins were analyzed as in Fig. 6. The levels of p30 produced relative to the uncapped full-length t2-2 reaction are shown below the lanes and represent the mean ± standard error for four experiments using the phosphor-imager for quantitation. Triangles mark the locations of CP and p21, and asterisks mark proteins synthesized from internal methionines in ORFs 1 and 2.

uncapped sgRNA transcripts (Fig. 8). However, the extent of the increase was smaller than for t2-2. Removing the 3′ ends decreased translation of uncapped sgRNA transcripts similarly to the decrease in t2-2Δ3′ translations, and capping the truncated sgRNA transcripts partially relieved the decrease indicating that the 3′CITE also functions on the sgRNAs (Fig. 8). To determine if a mutation in the KL could inactivate the 3′ CITE in sgRNA2, pNsg2-KLC was constructed. Transcripts from this plasmid contained changes in five nt in or near the KL that would decrease the number of potential consecutive base pairs from eight to three and from six to two for the predicted pairing sequences preceding the p21 and p19 start codons, respectively (Fig. 5). Mfold analysis of the 3′UTR of pNsg2-KLC predicted the same structure as for MNeSV (data not shown). The levels of p21 and p19 translation products from uncapped tNsg2-KLC were about four- and seven-fold lower, respectively, compared to products from tNsg2, and capping increased the translation rates (Fig. 8). Thus, the MNeSV genome has a 3′CITE that functions on gRNA and sgRNAs, and the KL is likely to be an important part of the 3′CITE.

Discussion

The completion of the sequence of MNeSV indicated that it is most closely related to tombusviruses. The nonstructural proteins are clearly most closely related to their dicot tombusviral homologs. Sequence comparisons, phylogenetic analysis, and RNA folding analysis of MNeSV RNA predict the formation of secondary structures and long-distance base-pairing interactions similar or identical to those previously shown to be involved with regulation of TBSV replication, sgRNA synthesis, and translation. These structures include TSD, SL5, and DSD located in the 5′UTR (Ray et al., 2003; Wu et al., 2001), IRE RII (Monkewich et al., 2005), sgRNA1 regulatory elements (AS1, SL1sg1, RS1) (Choi and White, 2002), sgRNA2 regulatory elements (AS2, RS2, DE, CE) (Lin and White, 2004), and the 3′ terminal hairpins containing the RSE (Fabian et al., 2003; Pogany et al., 2003) (Fig. 3A). The predicted secondary structure of the MNeSV 3′CITE differs from that for most tombusviruses, but it is located in the equivalent region of the 3′UTR and contains a loop sequence complementary to sequences in the TSD and 5′UTRs of the sgRNAs similar to TBSV.

The ability of the 3′CITE to function in vitro, the lack of infectivity by leaf rub inoculation, and the homology of the CP to those of necroviruses are characteristics of MNeSV that distinguish it from the dicot-infecting tombusviruses. Recent work indicates that, while vesicles form in MNeSV-infected maize cells, they are not the same as the multivesicular bodies typically found in dicot cells after tombusvirus infection (De Stradis et al., 2005). Of these differences, the activity of the 3′ CITE in WGE, the lack of transmission by rub inoculation, and cellular structures associated with virus infection in vivo may reflect the differences between monocot and dicot hosts rather than differences between MNeSV and tombusviruses. The closer relationship of the MNeSV CP to necroviruses than tombusviruses may be the result of recombination between a tombusvirus and a necrovirus since otherwise the CP ORF

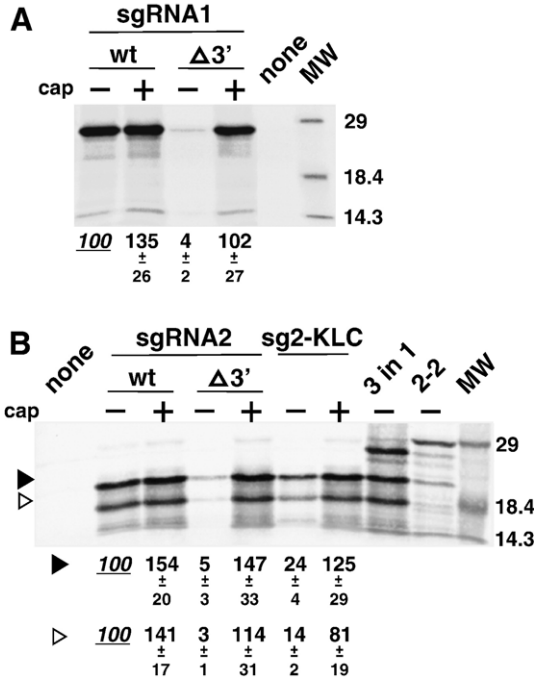

Fig. 8. Effects of ^{m}7GpppG caps and 3′ truncations on translation of sgRNA transcripts. Water (none) or 0.5 pmol of uncapped (−) t2-2 (2-2), uncapped and capped (+) full-length wild type (wt) tNsg1 and tNsg2, and tNsg2-KLC (sg2-KLC), or transcripts missing the 3′ 156 nt (Δ3′) were used to program WGE. For one reaction, equimolar amounts of uncapped t2-2, tNsg1, and tNsg2 were mixed, and 1.5 pmol of the mixture was translated by WGE (3 in 1). Sizes of molecular weight markers (MW) are on the right, and proteins were analyzed as in Fig. 6. (A) sgRNA1 transcripts. The levels of CP relative to uncapped tNsg1 are given below the lanes and represent the mean ± standard errors of four experiments. (B) sgRNA2 transcripts. The levels of p21 (black triangles) and p19 (open triangles) relative to uncapped tNsg2 are shown and represent the mean ± standard deviation of three experiments for wt and Δ3′ and two experiments for tNsg2-KLC.

would have had to undergo a deletion of the region encoding the protruding domain as well as extensive mutation within the remainder of the ORF to produce the MNeSV CP. It is interesting to note that ClustalW alignments of MNeSV RNA and dicot tombusvirus RNA sequences show that the borders of the MNeSV sequence with high tombusvirus homology surrounding the CP ORF precisely retain two tombusviral regulatory sequences; the first six nt of sgRNA1, which is a proposed base-pairing partner for the 3′CITE KL (Fig. 5), and RS-2 located 11 nt upstream of the sgRNA2 start site, the proposed base-pairing partner for AS-2 (Fig. 3A and data not shown). Retention of these sequences suggests that MNeSV uses the same or similar mechanisms as those identified in TBSV for regulating translation and sgRNA synthesis. Further support for placing MNeSV in the genus *Tombusvirus* comes from a phylogenetic analysis of the family Tombusviridae based on whole genome protein sequences that definitively placed MNeSV as a tombusvirus (Stuart et al., 2004). Taken together, the results indicate that, if MNeSV is not classified as a tombusvirus, it should be identified as the type member of a new genus within the family Tombusviridae.

The relative infectivity of the MNeSV transcripts with three different 5′ ends differed when tested in plants and protoplasts, and comparison with results from other tombusviral systems may help elucidate these results. Infectious transcripts have been made from cDNAs for six dicot-infecting tombusviruses, and all were initially tested for infectivity in plants. The *Cucumber necrosis virus* (CNV GenBank accession number M25270) cDNA produces a transcript initiating with GAAAU (Rochon and Johnston, 1991) which is similar to the MNeSV cDNA p2-2. cDNAs for TBSV-C (Hearne et al., 1990), *Cymbidium ringspot virus* (CyRSV GenBank accession number X15511) (Dalmay et al., 1993), *Artichoke mottle crinkle virus* (AMCV GenBank accession number X62493) (Tavazza et al., 1994), *Carnation Italian ringspot virus* GenBank accession number X85215 (Burgyan et al., 1996), and TBSV-P (GenBank accession number U80935) (Szittya et al., 2000) encode transcripts initiating with GGAAAU instead of the AGAAAU identified as the 5′ vRNA sequence (Burgyan et al., 1996; Szittya et al., 2000), deduced as the 5′ sequence from DI-RNAs (Dalmay et al., 1995; Finnen and Rochon, 1995) or by comparison to known tombusviral 5′ ends. Thus, the cDNAs for these viruses have a 5′ substitution similar to p8-6. As was found for seed inoculation of infectious MNeSV transcripts, relative infectivity of capped and uncapped transcripts of TBSV-C, CNV, CyRSV, and AMCV, the only transcripts tested this way, showed little or no difference (Dalmay et al., 1993; Hearne et al., 1990; Rochon and Johnston, 1991; Tavazza et al., 1994).

It was surprising that uncapped transcripts from p8-6 showed such poor replication in protoplasts since its 5′ end was similar to transcripts for five of the dicot-infecting tombusvirus cDNAs. There are several possible explanations for the effect of capping on t8-6 infectivity in protoplasts. A cap structure may protect the transcripts from 5′ exonuclease activity during the inoculation procedure, thereby increasing the number of intact RNA molecules available for translation and replication. Since there was a much smaller increase in protoplast infectivity produced by capping t2-2 and t5-6, it seems unlikely that this protection can account for the large capping effect on t8-6 infectivity in protoplasts but might explain the effect of capping on all transcripts in VPI infectivity (Fig. 4).

The lower infectivity of uncapped t8-6 may indicate that it is a poor template for replication or that it produces lower amounts of the RdRp from initial translation. The equally efficient synthesis of p30 and p89 from uncapped t8-6 and t2-2 in WGE (Scheets, data not shown) suggests that poor translation of the RdRp ORFs is not likely to explain the low infectivity. Conversely, capping t8-6 might increase its infectivity indirectly via translation. Since capped transcripts produced 1.5–3 times as much p30 and p89 as uncapped transcripts in WGE for both t2-2 (Fig. 6) and t8-6 (data not shown), a similar increase in initial RdRp synthesis in maize cells might increase initial replication enough to more rapidly overcome the disadvantage of having a less optimal 5′ end sequence, accumulating to high levels by 48 hpi. The 5′ ends of progeny derived from p8-6 transcripts are probably repaired during replication to the viral sequence as was seen for transcripts of a TBSV DI-RNA (Panavas and Nagy, 2003). The 5′ sequence of progeny vRNA from plants or protoplasts inoculated with transcripts was not determined. But if no repair occurred, all progeny from capped and uncapped t8-6 infections would look like uncapped t8-6, and replication would be expected to continue at the extremely poor rate seen at 48 hpi in protoplasts. The more similar infection rates of uncapped t2-2, t5-6, and t8-6 seen in plants suggest that the poor replication of uncapped t8-6 detected at 48 hpi in protoplasts is overcome soon after that since no difference in time of symptom appearance between the different transcripts was observed. Since the relative infectivity of capped and uncapped transcripts for the dicot-infecting tombusvirus cDNAs was not determined in protoplasts, it is not known whether the results seen with p8-6 transcripts are specific for MNeSV or are a general characteristic for tombusviruses.

Many positive strand RNA viruses that lack 5′ genome-linked proteins or caps have secondary structures that serve as translational enhancers such as the 3′CITE of TBSV (Fabian and White, 2004). Base pairing between residues in the TBSV 3′CITE and the TSD in the 5′UTR is required for the function of the TBSV 3′CITE, which is not active in WGE (Fabian and White, 2004; Wu and White, 1999). RNA secondary structure programs predicted no RNA secondary structure for MNeSV similar to the Y-shaped domain in the TBSV 3′UTR. This is not surprising considering the smaller size of the MNeSV 3′UTR and its lack of sequence similarity with the upstream portion of the TBSV 3′UTR. Nevertheless, the MNeSV 3′UTR contains a CITE which is active in WGE on gRNA and sgRNAs (Figs. 7 and 8). Both the 5′ and 3′ UTRs of MNeSV were most similar to those of CBLV, and the putative CBLV 3′CITE region (Fabian and White, 2004) is predicted by STAR to fold into a six bp–seven nt loop (data not shown) very similar to the terminus of the MNeSV 3′CITE (Fig. 2C). Interestingly, the seven nt loop in MNeSV has potential base-pairing partners in the 5′UTRs of both the gRNA and the sgRNAs (Fig. 5), and removal of this region abolished in vitro translational enhancing activity. It is possible that removing the 3′ terminal 156 nt greatly decreased

the stability of transcripts leading to decreased protein synthesis. However, if decreased transcript stability was the sole cause of decreased protein synthesis, the translation of both capped and uncapped truncated transcripts would be expected to decrease by similar amounts compared to their full-length transcripts. Instead, truncated capped transcripts were translated an order of magnitude more efficiently than truncated uncapped transcripts (Figs. 7 and 8). Thus, while the 3′UTR of MNeSV differs substantially in structure from that of TBSV, it is likely to carry a functionally similar translational enhancer.

The MNeSV 3′CITE shares some characteristics with other, well-studied, viral translational enhancers. BYDV-PAV, a luteovirus closely related to some members of the family Tombusviridae (Miller et al., 2002), has a 3′TE (BTE) consisting of a 109 nt cruciform structure (Guo et al., 2000) that base pairs with sequences in the 5′UTRs of gRNA and sgRNA1 to function in vitro (Guo et al., 2001). The MNeSV 3′CITE does not contain the highly conserved 18 nt sequence nor the secondary structure of BTE, and in contrast to BYDV (Allen et al., 1999), capped MNeSV gRNA transcripts do not show decreased infectivity in protoplasts. However, the smaller relative decrease in protein synthesis for the mutant transcript tNsg2-KLC compared to tNsg2Δ3′ and the stronger translation of capped full-length transcripts compared to capped Δ3′ transcripts are similar to BYDV. This suggests that the 3′UTR contains additional translation functions such as a poly(A) replacement similar to BYDV-PAV (Guo et al., 2000). After accounting for methionine content, the translation of equimolar amounts of gRNA and sgRNA transcripts in individual reactions indicates a translation efficiency of sgRNA2 > sgRNA1 > gRNA (Fig. 6). This may indicate that the 5′UTRs of the sgRNAs interact with the 3′CITE and/or translation factors more strongly than does the gRNA 5′ UTR as is the case for BYDV-PAV (Wang et al., 1999). Alternatively, the 5′–3′ interaction required for 3′CITE activity may form more readily on shorter RNAs. A stronger 3′CITE activity for sgRNAs than gRNA was also suggested by the smaller increases in translation produced by capping full-length sgRNAs than for capping t2-2 (Figs. 7 and 8). When equimolar amounts of gRNA and sgRNAs were translated together, the level of p30 synthesis was reduced to about one fourth the amount produced from translation of an equal amount of t2-2 alone. In contrast, the levels of sgRNA-encoded proteins were the same in mixed and single translations (3 in 1, Fig. 8 and data not shown). The decrease in gRNA translation in the mixed translations was not due to limiting amounts of initiation factors since sgRNA translations did not decrease. These results suggest that one or both MNeSV sgRNAs might inhibit initiation on gRNA as was seen with sgRNA2 inhibition on gRNA and sgRNA1 of BYDV-PAV (Wang et al., 1999).

The predicted structure of the MNeSV 3′CITE shares a general similarity with the predicted structure of the translational enhancer domain (TED) found in the 3′UTR of STNV in that they both contain a long stem loop with various bulges (van Lipzig et al., 2002). There is no sequence similarity or similarity in the sizes and locations of bulges and stem lengths, and, currently, there is no indication that the general structural similarity will be relevant at the functional level.

The construction of an infectious transcript cDNA of MNeSV provides a tool for future analysis of many different aspects of the MNeSV life cycle in a monocot host. Analysis of viral protein function is underway. Studies to determine the molecular basis of the difference in infectivity of t8-6 and t2-2 may shed light on viral replication processes in maize. In addition, chemical analysis of the MNeSV 3′CITE secondary structure, determination of long distance base-pairing with 5′UTRs in vivo and in vitro, and identification of interacting factors from WGE will provide insight into the mechanisms and regulation of the translational process. These experiments will allow comparisons with both the TBSV 3′CITE and the well-characterized 3′TEs of BYDV and STNV.

Materials and methods

Cloning and sequencing 5′ and 3′ ends of MNeSV vRNA

The 5′ end of the vRNA was cloned using the First Choice RLM-RACE kit (Ambion, Austin, TX) except that reverse transcription was performed with Thermoscript (Invitrogen, Carlsbad, CA) using MNeSV primer 5′RLM-RACE (Table 2) according to the manufacturer's instructions. vRNA was either directly ligated to the RNA oligomer (5′ RACE Adapter) from the RLM-RACE kit or was pretreated with CIP and TAP before RNA ligation. The cDNA was amplified with the 5′ RACE Inner Primer and the phosphorylated primer #106255 using Vent DNA polymerase (New England Biolabs, Boston, MA) according to the manufacturer's recommendations. After *Bam*HI digestion to cleave the 5′ RACE Inner Primer site, the fragment was gel-purified and cloned into the *Sma*I and *Bam*HI sites of Bluescript KS+ (Stratagene, La Jolla, CA). 5′ RACE (Invitrogen) was carried out according to the manufacturer's instructions using primer MNeSV2.1.1R for first-strand cDNA synthesis and MNESV2 for amplification of the C-tailed cDNA. cDNAs were cloned into pGEM-4z (Promega, Madison, WI) for sequence analysis.

The 3′ end was cloned using an anchored cDNA method (Weng and Xiong, 1995). T4 RNA ligase was used to ligate the phosphorylated DNA oligomer #785, which contains an *Mun*I site, to the 3′ end of the MNeSV vRNA and reverse transcribed with Thermoscript using the complementary primer #925. PCR amplification using primers #925 and 3′dsRNA, which binds upstream of the *Sal*I site in MNeSV, was followed by digestion with *Sal*I and *Mun*I, gel purification, and cloning into Bluescript SK+ digested with *Eco*RI and *Sal*I. These plasmids were named p3′-1, p3′-2 and p3′-3. Both strands of 5′ and 3′ cDNA plasmid inserts were sequenced.

Construction of infectious cDNA transcript plasmids

Six different full-length clones were made using standard cloning procedures (Sambrook et al., 1989). The 5′ end of MNeSV was placed downstream of a T7 RNA polymerase promoter by PCR amplification from a 5′ RLM-RACE cDNA using the primers MNeSV T7-1 or MNeSV T7-2 and 5′RLM-RACE. The DNA was digested with *Mfe*I and *Eco*RI, gel-

Table 2
Unique oligonucleotides used in cDNA constructions and primer extensions

Name	Sequence [a]	Sense [b]	Location [c]
#785	cttcaatttc*aattg*ggctgg(ddA) [d]		
#925	cctccagcc*caattg*aaattga		
3′dsRNA	TGAGGCATCTCGATTTCTCGGTGTC	+	3651–3675
5′RLM-RACE	AGCATTCGGTTGCGTCACTCTCGT	−	559–582
MNeSV2.1.1R	CCTCCTTACGCATCTTGAAC	−	521–540
MNESV2	g*gaattcc*ACCAGCGTTTGGCGAATAG	−	417–435
MNeSV T7-2	gaa*caattg*taatacgactcactata(g/A)GATATCGACCTGCCTGACCA	+	1–21
MNeSV T7-1	gaa*caattg*taatacgactcactataGATATCGACCTGCCTGACCA	+	2–21
MNeSV 3′SmaI	t*cccGGG*CTGCCCAAAGGCAATGTTC	−	4073–4094
MNe4076c	GGGCTGCCCAAAGGCAATG	−	4076–4094
T7/MNesg1	gtaatacgactcactataGACCAACAACTCGGCACAC	+	2488–2506
T7/MNesg2	gtaatacgactcactataGAACAAGACCAGTTCATGGATG	+	3314–3335
KLC	GC*GGTACC*gTGGCgttTCACtATGGTAATG	+	3932–3962
5′RO	ATACCAACTACGCCGGCTAG	−	35–54
sg1RO	TCTGCTGATCCTGTCATTTCC	−	2535–2554
sg2RO	TCGTTCCATGGCCTACTGAC	−	3350–3369

[a] Upper case letters represent MNeSV cDNA sequence, and lower case letters are non-MNeSV. Restriction sites are italicized, and the T7 RNA polymerase promoter is underlined.
[b] (+) Viral strand, (−) complementary strand.
[c] Numbering refers to (+) strand of GenBank sequence.
[d] Dideoxyadenosine.

purified and ligated into *Eco*RI digested pUC119. Clones (pT71A, pT722, and pT725) were selected that carried GATATC, GGATATC or AGATATC, respectively, immediately following the T7 promoter and with the remaining polylinker region 3′ of the insert. A unique *Sma*I site was placed at the 3′ end by amplifying DNA from p3′-3 and p3′-1 using the M13 Forward Sequencing Primer and phosphorylated MNeSV 3′ SmaI. After digestion with *Sal*I, the gel-purified fragments were cloned into pT71A, pT722, and pT725 that each contained a Klenow-filled *Hin*dIII end and *Sal*I sticky-end. Six different cDNAs with different 5′/3′ end combinations were digested with *Cla*I and *Sal*I for further insertions. Plasmids MNeSV2.1 and MNeSV2.2 (Louie et al., 2000) contain 2.5 and 1.67 kb inserts, respectively, that overlap by 248 bp. Both plasmids were linearized in the polylinker region with *Xba*I then digested with high concentrations of exonuclease III for 1 and 1.5 min at 37 °C to remove 250–500 nt of complementary strands followed by phenol/$CHCl_3$ extraction and precipitation (Schubert et al., 1988). MNeSV2.1 exonuclease III products were digested with *Cla*I, the MNeSV2.2 exonuclease III products were digested with *Sal*I, and the inserts consisting of dsDNA with long 3′ ssDNA tails were gel-purified, pooled, and precipitated. The fragments were dissolved in 50 mM NaCl, briefly heated, and allowed to anneal before ligating into the *Cla*I/*Sal*I-prepared 5′/3′ plasmids (Fig. 3). The 5′ and 3′ ends and 500–800 bases at the overlap junctions were sequenced for all clones, and the p8-6 and p2-2 inserts were sequenced completely.

Construction of sgRNA transcription plasmids

The 5′ ends of sgRNA1 and sgRNA2 were placed downstream of a T7 RNA polymerase promoter using phosphorylated oligos T7/MNesg1 or T7/MNesg2 and MNe4076c to amplify regions of p2-2 using Vent DNA polymerase, and the fragments were ligated to *Sma*I-digested pUC18. The resulting clones were named pNsg1 and pNsg2. To produce pNsg2-KLC, the M13 Reverse Sequencing Primer (−48) (New England Biolabs) and KLC were used to amplify the 3′ end of pNsg2 using Vent polymerase. After digestion with *Kpn*I and gel purification, the 160 bp fragment was ligated into the large fragment of pNsg2 which was digested with *Kpn*I and dephosphorylated. All sgRNA cDNA inserts were completely sequenced.

Primer extension analysis

The 5′ ends of sgRNAs were mapped by primer extension with Thermoscript reverse transcriptase (Scheets, 2000; Wang and Simon, 1997). Total RNA (3 μg) from healthy or MNeSV-infected maize plants or 0.5 μg of t8-6 (see below for synthesis) was annealed to 1 pmol of ^{33}P-labeled oligonucleotide sg1RO or sg2RO and reacted as described using 11 units of Thermoscript. One twelfth of each primer extension reaction was separated on an 8% polyacrylamide, 8 M urea sequencing gel along with dideoxy-termination sequencing reactions (Sequenase kit, Amersham, Piscataway, NJ) of p8-6 using the same radiolabeled primers. Primer extension reactions of vRNA contained 0.2 μg vRNA and radiolabeled 5′RO with a sequencing ladder generated from a 5′ RLM-RACE plasmid. The dried gels were exposed to a phosphorimager (BioRad, Hercules, CA).

Protoplast inoculations and analysis

Capped transcripts were synthesized using the mMessage mMachine kit (Ambion), and uncapped transcripts were synthesized as in Scheets (2000). Protoplast inoculations were performed as in Scheets (2000). Briefly, BMS suspension culture protoplasts ($1–1.5 \times 10^6$) were inoculated with 10 μg of transcripts or vRNA using polyethylene glycol, and washed

protoplasts were incubated in growth media with sampling at 0, 24, and 48 h. Samples for RNA and CP quantitation were prepared and analyzed by Northern blotting of agarose gels and PAS-ELISA, respectively (Scheets, 2000), except that RNA probes were synthesized from p3′-1 linearized with *Sal*I and rabbit antiserum to MNeSV (Louie et al., 2000) was used in the PAS-ELISA.

Maize infectivity assays

Capped transcripts for seed inoculations were synthesized using the mMessage mMachine kit (Ambion), and uncapped transcripts were synthesized with the same kit by substituting a solution containing 10 mM each of ATP, GTP, CTP, and UTP for the 2× NTP/CAP mixture. Seeds of the sweet corn variety Spirit were inoculated by vascular puncture (Redinbaugh et al., 2001). RNAs were quantitated using Ribogreen (Molecular Probes, Eugene, OR) (Jones et al., 1998) and adjusted to the same concentrations. Transcript RNA (0.5 to 1.1 μg in water) was pipetted onto a presoaked seed and immediately inoculated to control for exposure to RNases on seed surfaces. Non-inoculated plants served as negative controls, and positive controls were inoculated with extract from MNeSV-infected maize leaves ground in 10 mM potassium phosphate, pH 7. Plants were scored for symptoms twice between 6 and 20 days after inoculation.

In vitro translations with wheat germ extract (WGE)

Capped and uncapped RNAs were made from full-length (*Sma*I-linearized) or truncated (*Asp718*I-linearized) templates of p2-2, pNsg1, pNsg2, and full-length pNsg2-KLC. Translation reactions (25 μl) contained 0.5 pmol RNA, 10 μCi of ^{35}S-methionine, 130 mM potassium acetate, and 50% WGE (Promega). For some experiments, 0.5 pmol of t2-2, tNsg1, and tNsg2 were mixed and used in the same 25 μl reaction. One-fifth of each reaction was heat-denatured, separated on a 12% acrylamide Laemmli gel with a 6% stacking gel, and electroblotted to nitrocellulose (Bolt and Mahoney, 1997). ^{14}C-labeled proteins (Invitrogen) were used as molecular weight markers. Dried blots were exposed to a phosphorimager and analyzed with MultiAnalyst (BioRad) or OptiQuant (Perkin Elmer, Wellesley, MA) software.

Computer analysis

Sequence data were analyzed using Sequencher 3.1 (Gene Codes, Ann Arbor, MI), and the ClustalW program in MacVector 7.0 (Accelrys, San Diego, CA) was used for protein and RNA alignments. The 5′ and 3′ UTRs were analyzed with mfold (Zuker, 2003) online at http://www.bioinfo.rpi.edu/applications/mfold/old/rna/form1.cgi using both the version 3.1 free energy parameters (Mathews et al., 1999) which are fixed at 37 °C, and version 2.3 free energy parameters (Walter et al., 1994) at 28 °C and 37 °C. Folding predictions using the STAR program (v. 4) (Gultyaev et al., 1995) were performed using the greedy, stochastic, and genetic algorithms.

Acknowledgments

This research was supported by a grant from NSF (0440916). We thank Kristen Willie and John Abt for expert technical assistance. DNA sequencing was performed by the Recombinant DNA/Protein Resource Facility at Oklahoma State University and the Plant-Microbe Genomics Facility at Ohio State University. Mention of trade names or commercial products is made solely for the purpose of providing specific information and does not imply recommendation or endorsement by the U.S. Department of Agriculture.

References

Allen, E.M., Wang, S., Miller, W.A., 1999. *Barley yellow dwarf virus* RNA requires a cap-independent translation sequence because it lacks a 5′ cap. Virology 253, 139–144. doi:10.1006/viro.1998.9507.

Bolt, M.W., Mahoney, P.A., 1997. High-efficiency blotting of proteins of diverse sizes following sodium dodecyl sulfate-polyacrylamide gel electrophoresis. Anal. Biochem. 247, 185–192. doi:10.1006/abio.1997.2061.

Burgyan, J., Rubino, L., Russo, M., 1991. De novo generation of *Cymbidium ringspot virus* defective interfering RNA. J. Gen. Virol. 72, 505–509.

Burgyan, J., Rubino, L., Russo, M., 1996. The 5′-terminal region of a tombusvirus genome determines the origin of multivesicular bodies. J. Gen. Virol. 77, 1967–1974.

Choi, I.-R., White, K.A., 2002. An RNA activator of subgenomic mRNA1 transcription in *Tomato bushy stunt virus*. J. Biol. Chem. 277, 3760–3766. doi:10.1074/jbc.M109067200.

Choi, I.-R., Ostrovsky, M., Zhang, G., White, K.A., 2001. Regulatory activity of distal and core RNA elements in tombusvirus subgenomic mRNA2 transcription. J. Biol. Chem. 276, 41761–41768. doi:10.1074/jbc.M106727200.

Chu, M., Desvoyes, B., Turina, M., Noad, R., Scholthof, H.B., 2000. Genetic dissection of *Tomato bushy stunt virus* p19-protein-mediated host-dependent symptom induction and systemic invasion. Virology 266, 79–87. doi:10.1006/viro.1999.0071.

Dalmay, T., Russo, M., Burgyan, J., 1993. Repair in vivo of altered 3′ terminus of *Cymbidium ringspot tombusvirus* RNA. Virology 192, 551–555. doi:10.1006/viro.1993.1071.

Dalmay, T., Szittya, G., Burgyan, J., 1995. Generation of defective interfering RNA dimers of *Cymbidium ringspot tombusvirus*. Virology 207, 510–517. doi:10.1006/viro.1995.1111.

Danthinne, X., Seurinck, J., Meulewaeter, F., Van Montagu, M., Cornelissen, M., 1993. The 3′ untranslated region of *Satellite tobacco necrosis virus*-RNA stimulates translation in vitro. Mol. Cell. Biol. 13, 3340–3349.

De Stradis, A., Redinbaugh, M.G., Abt, J.J., Martelli, C.P., 2005. Ultrastructure of *Maize necrotic streak virus* infections. J. Plant Path. 87, 213–221.

Fabian, M.R., White, K.A., 2004. 5′–3′ RNA–RNA interaction facilitates cap- and poly(a) tail-independent translation of *Tomato bushy stunt virus* mRNA: a potential common mechanism for Tombusviridae. J. Biol. Chem. 279, 28862–28872. doi:10.1074/jbc.M401272200.

Fabian, M.R., Na, H., Ray, D., White, K.A., 2003. 3′-terminal RNA secondary structures are important for accumulation of *Tomato bushy stunt virus* DI RNAs. Virology 313, 567–580. doi:10.1016/S0042-6822(03)00349-0.

Finnen, R.L., Rochon, D.M., 1995. Characterization and biological activity of DI RNA dimers formed during *Cucumber necrosis virus* coinfections. Virology 207, 282–286. doi:10.1006/viro.1995.1078.

Gultyaev, A.P., van Batenburg, F.H., Pleij, C.W., 1995. The computer simulation of RNA folding pathways using a genetic algorithm. J. Mol. Biol. 250, 37–51. doi:10.1006/jmbi.1995.0356.

Guo, L., Allen, E.M., Miller, W.A., 2000. Structure and function of a cap-independent translation element that functions in either the 3′ or the 5′ untranslated region. RNA 6, 1808–1820.

Guo, L., Allen, E.M., Miller, W.A., 2001. Base-pairing between untranslated regions facilitates translation of uncapped, nonpolyadenylated viral RNA. Mol. Cell 7, 1103–1109. doi:10.1016/S1097-2765(01)00252-0.

Havelda, Z., Hornyik, C., Crescenzi, A., Burgyan, J., 2003. In situ characterization of *Cymbidium ringspot tombusvirus* infection-induced post-transcriptional gene silencing in *Nicotiana benthamiana*. J. Virol. 77, 6082–6086. doi:10.1128/JVI.77.10.6082-6086.2003.

Hearne, P.Q., Knorr, D.A., Hillman, B.I., Morris, T.J., 1990. The complete genome structure and synthesis of infectious RNA from clones of *Tomato bushy stunt virus*. Virology 177, 141–151. doi:10.1016/0042-6822(90)90468-7.

Jones, L.J., Yue, S.T., Cheung, C.Y., Singer, V.L., 1998. RNA quantitation by fluorescence-based solution assay: Ribogreen reagent characterization. Anal. Biochem. 265, 368–374. doi:10.1006/abio.1998.2914.

Kawaguchi, R., Bailey-Serres, J., 2002. Regulation of translational initiation in plants. Curr. Opin. Plant Biol. 5, 460–465. doi:10.1016/S1369-5266(02)00290-X.

Koh, D.C.-Y., Liu, D.X., Wong, S.-M., 2002. A six-nucleotide segment within the 3′ untranslated region of *Hibiscus chlorotic ringspot virus* plays an essential role in translational enhancement. J. Virol. 76, 1144–1153. doi:10.1128/JVI.76.3.1144-1153.2002.

Lin, H.-X., White, K.A., 2004. A complex network of RNA–RNA interactions controls subgenomic mRNA transcription in a tombusvirus. EMBO J. 23, 3365–3374. doi:10.1038/sj.emboj.7600336.

Lommel, S.A., Martelli, G.P., Rubino, L., Russo, M., 2005a. Genus *Necrovirus*. In: Fauquet, C.M., Mayo, M.A., Maniloff, J., Desselberger, U., Ball, L.A. (Eds.), Virus Taxonomy: Classification and Nomenclature of Viruses. Eighth Report of the International Committee on Taxonomy of Viruses. Elsevier Academic Press, San Diego, pp. 926–929.

Lommel, S.A., Martelli, G.P., Rubino, L., Russo, M., 2005b. Genus *Tombusvirus*. In: Fauquet, C.M., Mayo, M.A., Maniloff, J., Desselberger, U., Ball, L.A. (Eds.), Virus Taxonomy: Classification and Nomenclature of Viruses. Eighth Report of the International Committee on Taxonomy of Viruses. Elsevier Academic Press, San Diego, pp. 914–917.

Louie, R., Redinbaugh, M., Gordon, D., Abt, J., Anderson, R., 2000. *Maize necrotic streak virus*, a new maize virus with similarity to species of the family Tombusviridae. Plant Dis. 84, 1133–1139.

Mathews, D.H., Sabina, J., Zuker, M., Turner, D.H., 1999. Expanded sequence dependence of thermodynamic parameters improves prediction of RNA secondary structure. J. Mol. Biol. 288, 911–940. doi:10.1006/jmbi.1999.2700.

McLean, M.A., Campbell, R.N., Hamilton, R.I., Rochon, D.M., 1994. Involvement of the *Cucumber necrosis virus* coat protein in the specificity of fungus transmission by *Olpidium bornovanus*. Virology 204 (2), 840–842. doi:10.1006/viro.1994.1604.

Meulewaeter, F., van Lipzig, R., Gultyaev, A.P., Pleij, C.W.A., Van Damme, D., Cornelissen, M., van Eldik, G., 2004. Conservation of RNA structures enables TNV and BYDV 5′ and 3′ elements to cooperate synergistically in cap-independent translation. Nucleic Acids Res. 32, 1721–1730. doi:10.1093/nar/gkh338.

Miller, W.A., Liu, S., Beckett, R., 2002. *Barley yellow dwarf virus*: luteoviridae or tombusviridae? Mol. Plant Pathol. 3, 177–183. doi:10.1046/j.1364-3703.2002.00112.x.

Mizumoto, H., Tatsuta, M., Kaido, M., Mise, K., Okuno, T., 2003. Cap-independent translational enhancement by the 3′ untranslated region of *Red clover necrotic mosaic virus* RNA1. J. Virol. 77, 12113–12121. doi:10.1128/JVI.77.22.12113-12121.2003.

Monkewich, S., Lin, H.-X., Fabian, M.R., Xu, W., Na, H., Ray, D., Chernysheva, O.A., Nagy, P.D., White, K.A., 2005. The p92 polymerase coding region contains an internal RNA element required at an early step in tombusvirus genome replication. J. Virol. 79, 4848–4858. doi:10.1128/JVI.79.8.4848-4858.2005.

Nagy, P.D., Pogany, J., 2000. Partial purification and characterization of *Cucumber necrosis virus* and *Tomato bushy stunt* virus RNA-dependent RNA polymerases: similarities and differences in template usage between tombusvirus and carmovirus RNA-dependent RNA polymerases. Virology 276, 279–288. doi:10.1006/viro.2000.0577.

Panavas, T., Nagy, P.D., 2003. Yeast as a model host to study replication and recombination of defective interfering RNA of *Tomato bushy stunt virus*. Virology 314, 315–325. doi:10.1016/S0042-6822(03)00436-7.

Panavas, T., Pogany, J., Nagy, P.D., 2002. Analysis of minimal promoter sequences for plus-strand synthesis by the *Cucumber necrosis virus* RNA-dependent RNA polymerase. Virology 296, 263–274. doi:10.1006/viro.2002. 1423.

Pantaleo, V., Rubino, L., Russo, M., 2003. Replication of *Carnation Italian ringspot virus* defective interfering RNA in *Saccharomyces cerevisiae*. J. Virol. 77, 2116–2123. doi:10.1128/JVI.77.3.2116-2123.2003.

Pogany, J., Fabian, M.R., White, K.A., Nagy, P.D., 2003. A replication silencer element in a plus-strand RNA virus. EMBO J. 22, 5602–5611. doi:10.1093/emboj/cdg523.

Pogany, J., White, K.A., Nagy, P.D., 2005. Specific binding of tombusvirus replication protein p33 to an internal replication element in the viral RNA is essential for replication. J. Virol. 79, 4859–4869. doi:10.1128/JVI.79. 8.4859-4869.2005.

Qiu, W., Park, J.W., Scholthof, H.B., 2002. Tombusvirus p19-mediated suppression of virus-induced gene silencing is controlled by genetic and dosage features that influence pathogenicity. MPMI 15, 269–280.

Qu, F., Morris, T.J., 2000. Cap-independent translational enhancement of *Turnip crinkle virus* genomic and subgenomic RNAs. J. Virol. 74, 1085–1093.

Ray, D., Wu, B., White, K.A., 2003. A second functional RNA domain in the 5′ UTR of the *Tomato bushy stunt virus* genome: intra- and interdomain interactions mediate viral RNA replication. RNA 9, 1232–1245. doi:10.1261/rna. 5630203.

Reade, R., Wu, Z., Rochon, D., 1999. Both RNA rearrangement and point mutation contribute to repair of defective chimeric viral genomes to form functional hybrid viruses in plants. Virology 258 (2), 217–231. doi:10.1006/viro. 1999.9726.

Redinbaugh, M.G., Louie, R., Ngwira, P., Edema, R., Gordon, D.T., Bisaro, D. M., 2001. Transmission of viral RNA and DNA to maize kernels by vascular puncture inoculation. J. Virol. Methods 98, 135–143. doi:10.1016/S0166-0934(01)00369-X.

Rochon, D.M., Johnston, J.C., 1991. Infectious transcripts from cloned *Cucumber necrosis virus* cDNA: evidence for a bifunctional subgenomic mRNA. Virology 181, 656–665. doi:10.1016/0042-6822(91)90899-M.

Sambrook, J., Fritsch, E.F., Maniatis, T. (Eds.), 1989. Molecular Cloning: A Laboratory Manual. Cold Spring Harbor Laboratory Press, Cold Spring Harbor.

Scheets, K., 2000. *Maize chlorotic mottle machlomovirus* expresses its coat protein from a 1.47-kb subgenomic RNA and makes a 0.34-kb subgenomic RNA. Virology 267, 90–101. doi:10.1006/viro.1999.0107.

Scholthof, H.B., Scholthof, K.B., Kikkert, M., Jackson, A.O., 1995. *Tomato bushy stunt virus* spread is regulated by two nested genes that function in cell-to-cell movement and host-dependent systemic invasion. Virology 213, 425–438. doi:10.1006/viro.1995.0015.

Scholthof, K.B., Scholthof, H.B., Jackson, A.O., 1995. The effect of defective interfering RNAs on the accumulation of *Tomato bushy stunt virus* proteins and implications for disease attenuation. Virology 211, 324–328. doi:10.1006/viro.1995.1410.

Schubert, M., Brayton, P.R., Meier, E., 1988. Fusion of DNA sequences without the use of shared restriction sites. Focus 10, 8–9.

Shen, R., Miller, W.A., 2004. The 3′ untranslated region of *Tobacco necrosis virus* RNA contains a *Barley yellow dwarf virus*-like cap-independent translation element. J. Virol. 78, 4655–4664. doi:10.1128/JVI.78.9.4655-4664. 2004.

Stuart, G., Moffett, K., Bozarth, R.F., 2004. A whole genome perspective on the phylogeny of the plant virus family Tombusviridae. Arch.Virol. 149, 1595. doi:10.1007/s00705-004-0298-7.

Szittya, G., Salamon, P., Burgyan, J., 2000. The complete nucleotide sequence and synthesis of infectious RNA of genomic and defective interfering RNAs of TBSV-P. Virus Res. 69, 131–136. doi:10.1016/S0168-1702(00)00178-7.

Tavazza, M., Lucioli, A., Calogero, A., Pay, A., Tavazza, R., 1994. Nucleotide sequence, genomic organization and synthesis of infectious transcripts from a full-length clone of *Artichoke mottle crinkle virus*. J. Gen. Virol. 75, 1515–1524.

Timmer, R.T., Benkowski, L.A., Schodin, D., Lax, S.R., Metz, A.M., Ravel, J.M., Browning, K.S., 1993. The 5′ and 3′ untranslated regions of *Satellite tobacco necrosis virus*-RNA affect translational efficiency and dependence on a 5′ cap structure. J. Biol. Chem. 268, 9504–9510.

van Lipzig, R., Gultyaev, A.P., Pleij, C.W.A., van Montagu, M., Cornelissen, M., Meulewaeter, F., 2002. The 5′ and 3′ extremities of the *Satellite tobacco*

necrosis virus translational enhancer domain contribute differentially to stimulation of translation. RNA 8, 229–236. doi:10.1017/S1355838201018076.

Walter, A.E., Turner, D.H., Kim, J., Lyttle, M.H., Muller, P., Mathews, D.H., Zuker, M., 1994. Coaxial stacking of helixes enhances binding of oligoribonucleotides and improves predictions of RNA folding. Proc. Natl. Acad. Sci. U. S. A. 91, 9218–9222.

Wang, J., Simon, A.E., 1997. Analysis of the two subgenomic RNA promoters for *Turnip crinkle virus* in vivo and in vitro. Virology 232, 174–186. doi:10.1006/viro.1997.8550.

Wang, S., Guo, L., Allen, E.M., Miller, W.A., 1999. A potential mechanism for selective control of cap-independent translation by a viral RNA sequence in *cis* and in *trans*. RNA 5, 728–738.

Weng, Z., Xiong, Z., 1995. A method for accurate determination of terminal sequences of viral genomic RNA. Genome Res. 5, 202–207.

White, K.A., Nagy, P.D., 2004. Advances in the molecular biology of tombusviruses: gene expression, genome replication, and recombination. Prog. Nucleic Acid Res. Mol. Biol. 78, 187–226.

Wu, B., White, K.A., 1999. A primary determinant of cap-independent translation is located in the 3′-proximal region of the *Tomato bushy stunt virus* genome. J. Virol. 73, 8982–8988.

Wu, B., Vanti, W.B., White, K.A., 2001. An RNA domain within the 5′ untranslated region of the *Tomato bushy stunt virus* genome modulates viral RNA replication. J. Mol. Biol. 305, 741–756. doi:10.1006/jmbi.2000.4298.

Zhang, G., Slowinski, V., White, K.A., 1999. Subgenomic mRNA regulation by a distal RNA element in a (+)-strand RNA virus. RNA 5, 550–561.

Zuker, M., 2003. Mfold web server for nucleic acid folding and hybridization prediction. Nucleic Acids Res. 31, 3406–3415. doi:10.1093/nar/gkg595.